

An Iterative Threshold Algorithm Based on Log-sum Norm Regularization for Magnetic Resonance Image Recovery

Lin Yu Wang, Ming Qi He*, Jian Hong Xiang, and Peng Fei Ye

Abstract—This paper considers the class of Iterative Shrinkage Threshold Algorithm (ISTA) to solve the linear inverse problem that occurs in magnetic resonance (MR) image recovery. The ISTA algorithm adheres to the principle of minimizing the L1 norm. This method can be considered as an extension of the classical gradient algorithm. However, it is known that the ISTA algorithm converges slowly, and the accuracy of the algorithm is not sufficient. In many MR image recovery problems, using non-convex log-sum norm minimization can often obtain better results than the l1-norm minimization. In this paper, we firstly transform the MR image recovery into a non-convex optimization problem with log-sum norm regularization and combine it with a faster global convergence method. Then a Log-sum generalized iterated shrinkage threshold algorithm (LISTA) for solving the MR image recovery problem is proposed. Finally, numerical experiments are conducted to show the superiority of our algorithm.

1. INTRODUCTION

MR image recovery plays a vital role in clinical diagnosis. However, at present, the quality of MR image recovery needs to be strengthened. Compressed sensing (CS) is a new sampling technique applied to MR imaging recovery. The CS first acquires a small amount of k-space data (also called Fourier coefficients) to shorten the image recovery time, then reconstructs the MR image from the undersampled data. Assuming the image is sparse, we can recover the image from a small number of Fourier coefficients. Therefore, we need to find an image that is sparse in the transform domain to fit the undersampled k-space data. We can transform the MR image by transforming domain (such as DCT, Fourier, wavelet), so that CS can be applied to MR image recovery. There have been some studies showing that the MR image restoration problem is a morbid inverse problem, so the commonly used image reconstruction method is to add regularization to the problem. MR image recovery based on compressed sensing mainly concerned with the problem of so-called sparseness constraint minimization, and image restoration is often achieved by sparse minimization. One difficulty with the sparse constraint minimization problem is the choice of minimized norm. In recent years, Daubechies et al. proposed iterative shrinkage thresholding algorithm (ISTA) [1] based on the L1 norm regularization problem and successfully applied it to MR image recovery. The ISTA idea is relatively simple. It only needs to determine the initial value of the algorithm, step size, and denoising operator, and achieve the convergence effect by the gradient descent. Then, under the framework of the ISTA algorithm, Beck and Teboulle proposed the Fast Iterative Shrinkage-Thresholding Algorithm [2] to improve the convergence speed of the algorithm. Based on ISTA algorithm, a two-step iterative shrinkage threshold algorithm is proposed in [3], which is also based on the idea of improving the algorithm speed. Inspired by the ISTA that solves the L1 regularization problem, Zuo et al. proposed a generalized iterative shrinkage thresholding algorithm (GISA) [4] to solve the Lp regularization problem. Compared with ISTA, GISA uses different methods

Received 3 November 2019, Accepted 2 January 2020, Scheduled 13 January 2020

* Corresponding author: Ming Qi He (hemingqi@hrbeu.edu.cn).

The authors are with the College of Information and Communication Engineering, Harbin Engineering University, Harbin 150001, China.

of contraction operator, while the iteration form is almost the same as ISTA. Then some scholars have made further improvement based on GISTA algorithm, and proposed FGISTA algorithm [5]. FGISTA algorithm improves the speed of GISTA algorithm, but the accuracy is decreased. Based on the p -norm, Chartrand and Yin proposed an Iterative Reweighted Least Squares (IRLS) algorithm [6]. Unlike gradient descent, the algorithm uses the least squares method to converge. Paper [7] proposes to apply $l_{\frac{1}{2}}$ norm to iterative threshold algorithm, which further extends the compressed sensing algorithm. Now, this kind of compressed sensing algorithm is widely used in various fields, such as image restoration [8–10] and MRI imaging [11], because of its strong scalability.

There are still a lot of studies on the problem of minimizing the norm. Some scholars have suggested in the literature [12–14] that the log-sum norm can effectively approximate the L0 norm and prove that the log-sum norm can also be used as a regularization term.

2. RELATED WORK

Previous studies of MR image recovery have shown that using L0 norm minimization usually yields good results, and it is designed to address the following minimization problems:

$$\min \frac{1}{2} \|\mathbf{y} - \mathbf{A}\mathbf{x}\|^2 + \lambda \|\mathbf{x}\|_0 \quad (1)$$

where \mathbf{y} is an $n \times 1$ vector, \mathbf{A} a sensing matrix, \mathbf{x} the the original signal (or image), and $\|\mathbf{x}\|_0$ simply counts the number of non-zero entries in \mathbf{x} . Unfortunately, the L0 norm is a non-convex non-continuous function, which makes the corresponding solution problem very cumbersome.

Since the L1 norm is a convex hull of L0 norm and has the property of continuity, many researchers have shifted the study to the L1 norm. It has been proved that the L1 norm minimization is equivalent to the L0 norm minimization when \mathbf{A} satisfies certain conditions [15, 16]. Unlike solving the L0 norm minimization, many algorithms seek the desire \mathbf{x} by solving the following convex optimization problem:

$$\min \frac{1}{2} \|\mathbf{y} - \mathbf{A}\mathbf{x}\|^2 + \lambda \|\mathbf{x}\|_1 \quad (2)$$

In solving [2], the fast iterative shrinkage-thresholding algorithm (FISTA) which is based on the gradient descent method makes smarter choices in the iterative process to obtain the ideal solution. In ISTA algorithm, Donoho proposed a soft threshold operator [16], which is defined as:

$$T_1(\mathbf{y}; \lambda) = \begin{cases} 0, & |\mathbf{y}| \leq \lambda \\ \text{sgn}(\mathbf{y})(|\mathbf{y}| - \lambda) & |\mathbf{y}| > \lambda \end{cases} \quad (3)$$

Based on the ISTA algorithm, FISTA improves the selection of the starting point and improves the convergence speed of ISTA algorithm. The difference between the two algorithms is the choice of the initial position.

To solve the L1 norm problem, the GISTA algorithm gives a model using the p -norm:

$$\min \frac{1}{2} (\mathbf{y} - \mathbf{A}\mathbf{x})^2 + \lambda \mathbf{x}^p \quad (4)$$

Like the traditional iterative threshold method, GISTA algorithm needs to approximate the convergence image by gradient descent. However, GISTA needs to define its p value according to different noise intensities and different images in order to get better reconstruction effect.

In order to solve the problem in Eq. (1), some researchers have proposed the optimization problem of the log-sum norm, which is expressed as:

$$\min \frac{1}{2} (\mathbf{y} - \mathbf{A}\mathbf{x})^2 + \lambda \log(\mathbf{x} + u) \quad (5)$$

It has been proved in [5] that when u is equal to 0, the log-sum norm is close to the L0 norm. Theoretical and experimental results also show that log-sum norms can yield solutions that are more sparse than the L1 norm in some cases. Compared with the L0 norm, although the log-sum norm is continuous, it loses its convexity relative to the L1 norm, which makes the log-sum regularization problem difficult to solve the convex optimization algorithm.

This paper mainly discusses the MR image recovery problem based on log-sum norm constraint. Based on the ISTA algorithm, a Log-sum generalized iterated shrinkage threshold algorithm (LISTA) for solving Equation (5) is presented.

So far, various algorithms have been proposed to minimize the norm in MR image recovery. The process of obtaining the sampled MR image can be expressed as:

$$\mathbf{y} = \mathbf{Ax} + \boldsymbol{\eta} \tag{6}$$

where \mathbf{A} is a sampling matrix or sensing matrix, \mathbf{x} the original image, $\boldsymbol{\eta}$ the noise, and \mathbf{y} the acquired compressed signal (or image). The MR image recovery problem is the process of recovering the ideal image \mathbf{x} from the compressed image \mathbf{y} . Since the sampling matrix \mathbf{A} is a highly ill-conditioned matrix, the problem is an ill-posed inverse problem, and a common method for solving ill-conditioned problems is to regularize it.

This paper mainly considers the MR image recovery problem based on log-sum norm regularization:

$$\min \frac{1}{2} \|\mathbf{y} - \mathbf{Ax}\|_2 + \sum_{i=1}^n \lambda \log(|x_i| + \varepsilon) \tag{7}$$

where $\frac{1}{2} \|\mathbf{y} - \mathbf{Ax}\|_2$ is often referred to as the data fitting term, and $\lambda \log(|x_i| + \varepsilon)$ is the penalty term. ε acts as a regularization, balancing the value of the function $f(\mathbf{x})$ when \mathbf{x} is too small, and it usually takes from 0.01 to 0.001. LISTA algorithm adopts the idea of the ISTA algorithm based on the log-sum norm as the penalty term, and its core is to find a contraction operator similar to the iterative threshold class algorithm.

3. MAIN RESULTS

The core of the ISTA algorithm is the gradient descent method. The unconstrained optimization problem is as follows:

$$\min_x \{F(\mathbf{x}) = f(\mathbf{x})\} \tag{8}$$

where $f(\mathbf{x})$ is the formula $\frac{1}{2} \|\mathbf{y} - \mathbf{Ax}\|_2$. Assume that $f(\mathbf{x})$ is continuously differentiable, if there is a small enough value $t_k > 0$ such that $x_{k+1} = x_k - t \nabla F(x_k)$, then:

$$F(x_k) \geq F(x_{k+1}) \tag{9}$$

The x_k value corresponding to the minimum value of the function $f(\mathbf{x})$ can be obtained by iterating through the following steps:

$$x_k = x_{k-1} - t_k \nabla f(x_{k-1}), \quad x_0 \in R^n \tag{10}$$

The ISTA algorithm assumes that $f(\mathbf{x})$ satisfies the Lipschitz continuous condition, that is, the derivative of $f(\mathbf{x})$ has a lower bound, and the minimum lower bound is called the Lipschitz constant $L(f)$. At this time, for any $L \geq L(f)$, there are:

$$f(\mathbf{x}) \leq f(\mathbf{y}) + \langle \mathbf{x} - \mathbf{y}, \nabla f(\mathbf{y}) \rangle + \frac{L}{2} \|\mathbf{x} - \mathbf{y}\|^2 \quad \mathbf{x}, \mathbf{y} \in R^n \tag{11}$$

Based on Eq. (11), the function value can be approximated near point x_k :

$$\hat{f}(\mathbf{x}, x_k) = f(x_k) + \langle \nabla f(x_k), \mathbf{x} - x_k \rangle + \frac{L}{2} \|\mathbf{x} - x_k\|^2 \tag{12}$$

Adopting this same basic gradient idea to the nonsmooth L1 regularized problem:

$$\min_x \{F(\mathbf{x}) = f(\mathbf{x}) + \lambda \|\mathbf{x}\|_1\} \tag{13}$$

After bringing the function into the penalty, the value of the function can be approximated by the point x_k :

$$\hat{f}(\mathbf{x}, x_k) = f(x_k) + \langle \nabla f(x_k), \mathbf{x} - x_k \rangle + \frac{L}{2} \|\mathbf{x} - x_k\|^2 + \lambda \|\mathbf{x}\|_1 \tag{14}$$

In each iteration of gradient descent, the approximation function of point x_{k-1} takes the minimum point as the starting point x_k of the next iteration:

$$x_k = \arg \min_x \left\{ f(x_{k-1}) + \langle \mathbf{x} - x_{k-1}, \nabla f(x_{k-1}) \rangle + \frac{1}{2t_k} \|\mathbf{x} - x_{k-1}\|^2 + \lambda \|\mathbf{x}\|_1 \right\} \quad (15)$$

After ignoring constant terms, Eq. (15) can be rewritten as:

$$x_k = \arg \min_x \left\{ \frac{1}{2t_k} \|\mathbf{x} - (x_{k-1} - t_k \nabla f(x_{k-1}))\|^2 + \lambda \|\mathbf{x}\|_1 \right\} \quad (16)$$

Inspired by ISTA, we propose a generalized shrinkage thresholding operator to solve the log-sum minimization problem in Eq. (5) by modifying the shrinkage rules. We convert the L1 norm regularization into a log-sum norm regularization problem and simplify it based on Eq. (16), which is expressed as:

$$x_k = \arg \min_x \left\{ \frac{1}{2t_k} \|\mathbf{x} - (x_{k-1} - t_k \nabla f(x_{k-1}))\|^2 + \sum_{i=1}^n \lambda \log(|x_i| + \varepsilon) \right\} \quad (17)$$

In order to facilitate the analysis of the change in the concavity, we turn the above formula into the simplest logsum norm minimization problem:

$$\min \frac{1}{2t_k} (\mathbf{x} - \mathbf{y})^2 + \lambda \log(\mathbf{x} + \varepsilon) \quad (18)$$

where t_k is the step size and is generally taken as 1. λ is known as regularization strength, and its value range is generally $(0, 1]$. If $\mathbf{y} > 0$, the solution to Eq. (18) should fall into the range of $[0, \mathbf{y}]$. If $\mathbf{y} < 0$, the solution into the range of $[\mathbf{y}, 0]$. Without loss of generality, in the paper we only consider the case $\mathbf{y} > 0$, and we set $t_k = 1$ and $\lambda = 0.3$. In Fig. 1, we take four different values for \mathbf{y} . It can be seen from Fig. 1 that there is a threshold $\tau_{\log\text{-sum}}$. When $\mathbf{y} < \tau_{\log\text{-sum}}$, then 0 is the value of \mathbf{x} corresponding to the global minimum. When $\mathbf{y} > \tau_{\log\text{-sum}}$, the local minimum and zero values need to be compared.

For the non-convex problem, if the contraction rule of the ISTA algorithm is directly adopted, \mathbf{x} can generally only shrink to the local minimum rather than the global minimum. Therefore, we need to set a threshold $\tau_{\log\text{-sum}}$ to judge various situations. First, we need to determine if the function has a local minimum.

We can analyze the convergence of the function by the first derivative and the second derivative of $f(\mathbf{x})$.

$$\begin{aligned} f'(\mathbf{x}) &= \mathbf{x} - \mathbf{y} + t_k \lambda \frac{1}{\mathbf{x} + \varepsilon} \\ f''(\mathbf{x}) &= 1 - \lambda t_k \frac{1}{(\mathbf{x} + \varepsilon)^2} \end{aligned} \quad (19)$$

We can get this inflection point by the second derivative of the function $f(\mathbf{x})$. The inflection point coordinates are $x^\lambda = \sqrt{\lambda t_k - \varepsilon}$. We can see from Fig. 1 that when $\mathbf{x} > x^\lambda$, the function $f(\mathbf{x})$ is concave; otherwise, it is convex. If the function has a local minimum, $f'(x^\lambda) \leq 0$. Based on this, we can get a threshold by the following formula.

$$f'(x^\lambda) = x^\lambda - \mathbf{y} + t_k \lambda \frac{1}{x^\lambda} = 0 \quad (20)$$

We can get the threshold of \mathbf{y} :

$$\tau_{\lambda t_k} = \sqrt{\lambda t_k - \varepsilon} + \frac{\lambda t_k}{\sqrt{\lambda t_k - \varepsilon}} \quad (21)$$

However, it is easy to find through c in Fig. 1: even if the function $f(\mathbf{x})$ has a local minimum, it needs to compare the size with $f(0)$ to determine the global minimum. As shown in Fig. 1(d), when \mathbf{y} exceeds a certain threshold, the local minimum of the function is the global minimum. Assuming that

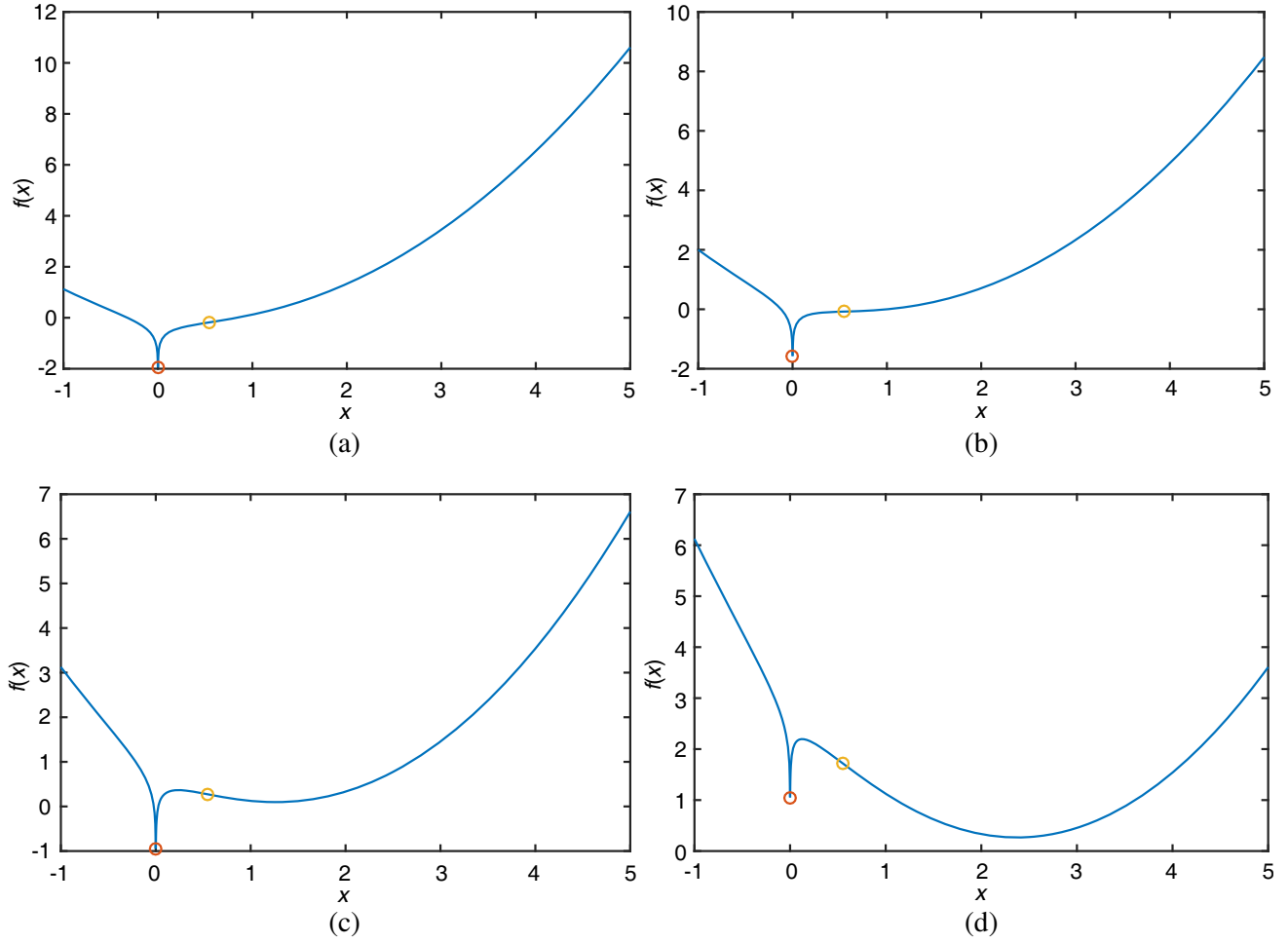


Figure 1. Plots of the function $f(\mathbf{x})$ in Eq. (18) with different values of \mathbf{y} : (a) $\mathbf{y} = 0.5$, (b) $\mathbf{y} = 1$, (c) $\mathbf{y} = 1.5$, (d) $\mathbf{y} = 2.5$.

the critical point is \tilde{x} , an approximate estimate of \tilde{x} can be obtained by the formula $f(\tilde{x}) = \lim_{x \rightarrow 0} f(\mathbf{x})$ and $f'(\tilde{x}) = 0$:

$$\begin{cases} \tilde{x} - \tau_x + t_k \lambda \frac{1}{\tilde{x} + \varepsilon} = 0 \\ f(\tilde{x}) = \lim_{x \rightarrow 0} f(\mathbf{x}) \end{cases} \quad (22)$$

However, the solution to this equation is a transcendental equation, and we can only get an approximate solution through matlab. Based on this, we can get an approximation of estimate $\tilde{x} \approx \frac{\sqrt{\varepsilon^2 + 8t_k \lambda} - \varepsilon}{2}$. The regularization factor ε is generally taken as $[0.01, 0.001]$, so its quadratic square can be ignored. Therefore, $\tilde{x} \approx \sqrt{2t_k \lambda} - \varepsilon/2$. τ_x corresponding to x is taken as its threshold. Then the approximate estimate of the threshold $\tilde{\tau}_x$ is:

$$\tilde{\tau}_x = \sqrt{2t_k \lambda} - \frac{\varepsilon}{2} + \frac{t_k \lambda}{\sqrt{2t_k \lambda} + \varepsilon/2} \quad (23)$$

Now we can draw conclusions. When \mathbf{y} is greater than $\tau_{\log\text{-sum}}$, we can judge that function $f(\mathbf{x})$ has a local minimum value. When \mathbf{y} is greater than $\tilde{\tau}_x$, the local minimum value is the global minimum. We can get the iterative contraction rules (LST operator) corresponding to the LISTA algorithm as shown in the left of Table 1, where J is the number of iterations with decreasing gradient when calculating the iterative threshold compression operator. When J is too large, the LST operator may not reach the

Table 1. The left is the log-sum contraction operator corresponding to the LISTA algorithm, which is LST. The right is the total LISTA algorithm step.

Algorithm 1 (LST)	Algorithm 2 (LISTA)
Input: $\mathbf{y}, \lambda, t_k, J$	Input: $\mathbf{y}, \lambda, t_k, J, \text{iter}$
Step 1 $\tilde{\tau}_x = \sqrt{2t_k\lambda} + t_k\lambda/\sqrt{2t_k\lambda} + \varepsilon$	Step 1 Initialize $\mathbf{x}^0 = \mathbf{y}, \mathbf{z}^0 = \mathbf{x}^0$
Step 2 if $\mathbf{y} < \tilde{\tau}_x$	Step 2 for $k = 1$: iter
Step 3 $T_{LST}(\mathbf{y}\lambda) = 0$	Step 3 $\mathbf{y} = \mathbf{z}^{k-1} - t^k \mathbf{A}^T (\mathbf{A} \mathbf{z}^{k-1} - \mathbf{y})$
Step 4 else	Step 4 $\mathbf{x}^k = LST(\mathbf{y}, \lambda, t_k, J)$
Step 5 $\mathbf{x}^k = \mathbf{y} $	Step 5 $l^k = (1 + \sqrt{1 + 4(l^{k-1})^2})/2$
Step 6 Iterate on $k = 0, 1, \dots, J$	Step 6 $\mathbf{z}^k = \mathbf{x}^k + \frac{l^{k-1}-1}{l^k}(\mathbf{x}^k - \mathbf{x}^{k-1})$
Step 7 $\mathbf{x}^{k+1} = \mathbf{y} - \lambda t_k (\mathbf{x}^k)^{-1}$	Step 7 $\mathbf{x} = \mathbf{x}^{iter}$
Step 8 $k = k + 1$	Step 8 end
Step 9 $T_{LST}(\mathbf{y}\lambda) = \text{sgn}(\mathbf{y})x^k$	Output: \mathbf{x}
Step 10 end	
Output: $T_{LST}(\mathbf{y}\lambda)$	

minimum value. When J is too small, the total number of iterations of LISTA algorithm will increase, resulting in the increase of the total time.

The above is the operator that selects the minimum value, and the body of the LISTA algorithm is similar to the ISTA algorithm. We introduce the above iterative contraction operator based on the ISTA algorithm and add the acceleration operator of the FISTA algorithm to the LISTA algorithm. The corresponding algorithm is shown in the right of Table 1.

4. NUMERICAL EXAMPLE

In this section, we will present numerical results to illustrate the efficiency of our proposed algorithm. We firstly compare the efficiencies of the LISTA algorithm in radial sampling matrix at different sampling rates. In the second subsection, we will compare FISTA, GISTA, LISTA, then we also select several state of the art methods for comparisons. In the last subsection, we will analyze the convergence of different algorithms under different iterations. The test MR images are mainly taken from the medical image library, shown in Fig. 2, and we add a Gaussian noise with a standard deviation of 1e-2 to the test.

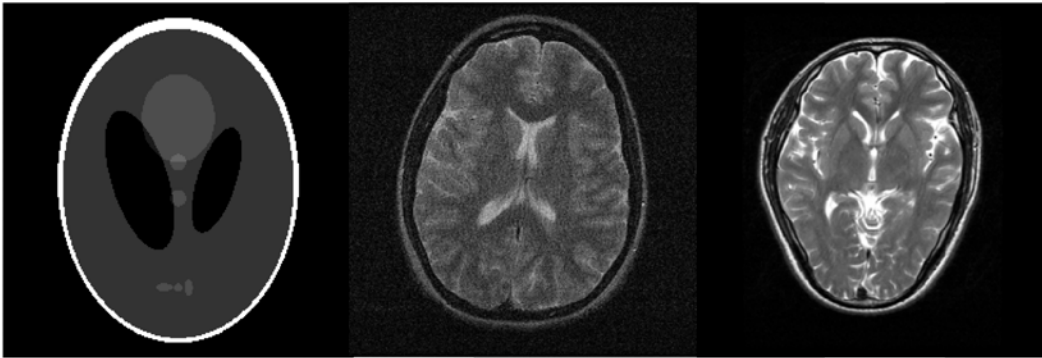


Figure 2. Original images. All the image size are $512 * 512$.

4.1. Evaluation Criterion

In this subsection, we use SSIM, peak signal-noise ratio (PSNR), and running time to evaluate the quality of restoration, which are defined as:

$$\text{MSE} = \|\mathbf{x} - \hat{\mathbf{x}}\|_2 / (M \times N) \quad (24)$$

$$\text{PSNR} = 10 \lg(255^2 / \text{MSE}) \quad (25)$$

$$\text{SSIM}(p, q) = \frac{(2\mu_p\mu_q + c_1)(2\sigma_{pq} + c_2)}{(\mu_p^2 + \mu_q^2 + c_1)(\sigma_p^2 + \sigma_q^2 + c_2)} \quad (26)$$

where $\hat{\mathbf{x}}$ and \mathbf{x} denote the original and restored image respectively, and M and N represent the length and width of the picture. We also consider the running time of every algorithm. SSIM is a new indicator to measure the structural similarity between two images. In image restoration, the larger the SSIM value is, the better the image restoration quality is. μ_p is the mean of image p , and μ_q is the mean of image q . $c_1 = k_1L$ and $c_2 = k_2L$, in which k_1 is 0.01, and k_2 is 0.03. L is the dynamic range of pixel values. σ_p and σ_q are the variance of image. σ_{pq} is the covariance between two images.

We conduct some experiments to illustrate the superiority of the LISTA algorithm in MR image recovery. In the selection of parameters, we uniformly set the step size t_k to 0.5. The range of regularization parameters λ is generally $(0, 1]$. In past experiments, the selection of regularization parameters λ based on changes in noise intensity could yield better MR image recovery results, so we set the regularization parameter λ to 1 under this low noise condition. For GISA algorithm, we choose $p = 0.8$ (the p value is also chosen in the original paper.) for the comparison. For FISTA algorithm, the regularization strength is the same as LISTA algorithm, which is taken as 1. For fairness, according to other references, we can obtain satisfactory results by uniformly selecting $J = 2$ or 3, so we set $J = 2$. All experiments are operated under Windows 10 and MATLAB R2016a with the platform of Intel (R) Core (TM) i5-7th Gen CPU@2.50 GHz 2.50 GHz.

Next, we will carry out our experiments from three aspects: 1) reconstruct the same MR image at different sample rates. 2) analyze the peak signal to noise ratio (PSNR) of different algorithms. 3) analyze the convergence of the algorithm under certain noise conditions.

4.2. Performance Evaluation of Different Sample Rates for MR Image Recovery under the Same Conditions

First, we display the original image of the MR image. The selected sampling matrix is a radial sampling matrix under the Fourier domain. In the experiment, the sampling rate of the matrix is 30%; the obtained reconstructed image PSNR is 38.44 dB; reconstruction time is 0.712 seconds. The result is shown in Fig. 3. From Fig. 3, we can find that under the 30% sampling matrix, our algorithm can reconstruct the MR image effectively.

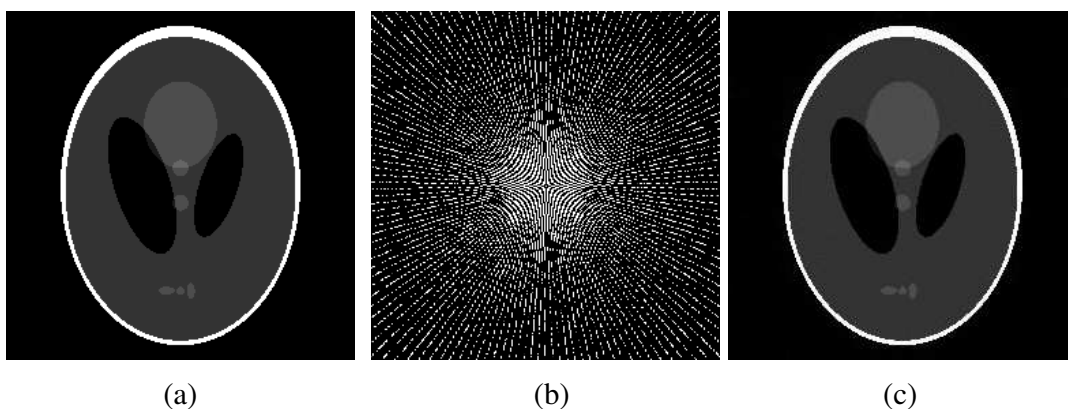


Figure 3. The MR image recovery effect of the LISTA algorithm at 30% sampling. (a) Original image. (b) Sampling matrix. (c) The reconstructed image.

Table 2. Comparison of PSNR and time after restoration of MR images of LISTA algorithm under different sampling matrices.

Sampling Rate	PSNR (dB)	SSIM (%)	time (s)
20%	28.96	65.88	0.65
30%	38.44	95.54	0.71
40%	44.20	98.05	0.74
50%	47.58	98.90	0.75

From Table 2 we can see that when the sampling rate is greater than 30%, LISTA algorithm works well on reconstructing MR images, with PSNR greater than 38 dB and SSIM greater than 90%. As the sampling rate increases, the effect of reconstructing the MR image is better. It can be seen from Table 2 that an increase in the sampling rate will increase the time. However, this result verifies the superiority of compressed sensing compared to Nyquist sampling. The LISTA algorithm can reconstruct MR images with superior quality by reducing the sampling rate.

4.3. Performance Evaluation of Different Algorithms

In order to eliminate the influence of random factors on the algorithm results, we use the 30% sampling matrix to test different images. The parameter selection is the same as 4.1. We use GISTA, FISTA and LISTA algorithms to perform the recovery of PSNR of the MR image after testing 100 times. The experimental picture is shown in Fig. 4. The specific data are shown in Table 3. It can be seen from

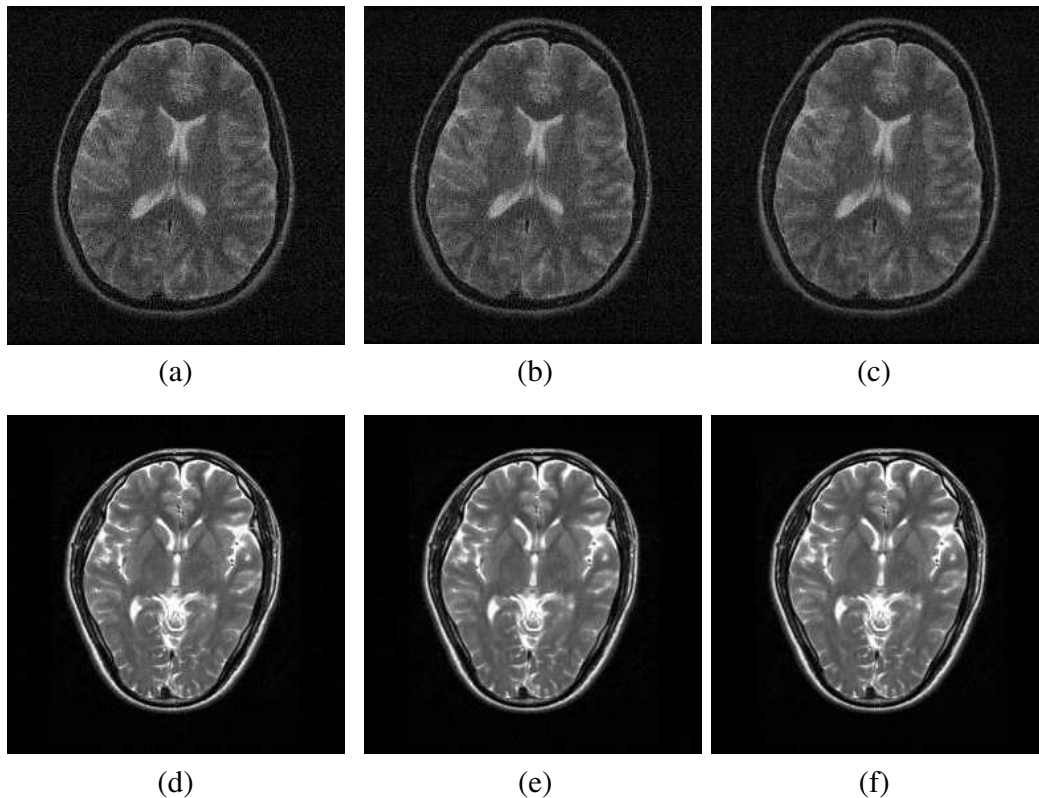


Figure 4. MR image recovery results at 30% sampling. (a) Image 1 FISTA recovery results. (b) Image 1 GISTA recovery results. (c) Image 1 LISTA recovery results. (d) Image 2 FISTA recovery results. (e) Image 2 GISTA recovery results. (f) Image 2 LISTA recovery results.

Table 3. Comparison of effects of LISTA, GISTA and FISTA algorithms in MR image reconstruction.

image	algorithm	PSNR (dB)	SSIM (%)	time (s)
image 1	FISTA	27.08	0.861	0.648
	GISTA	28.00	0.931	0.689
	LISTA	28.94	0.941	0.734
image 2	FISTA	35.20	0.922	0.870
	GISTA	36.06	0.932	0.880
	LISTA	36.08	0.944	0.877

Table 3 that the algorithm effect of LISTA is good for different algorithms. These experiments show that the LISTA algorithm is more accurate than other algorithms under low noise conditions.

Combined with Table 3 and Fig. 4, FISTA is less accurate than other algorithms but with less time, and GISTA algorithm is somewhere in between. The accuracy of the proposed LISTA algorithm has been improved, both in SSIM and PSNR. We can see that LISTA algorithm has reached the standard of the iterative threshold class algorithm and even surpassed the accuracy of some iterative threshold algorithms.

4.4. Performance Evaluation of Convergence of Different Algorithms

In this section, we compare PSNR changes in different algorithms as the number of iterations increases. The selected MR images are identical and are the third image of Fig. 2. In the parameter selection, we set J for each type of algorithm to 2, set the step size t_k to 1, and set the regularization parameter λ to 1. The standard deviation of the added noise is 0.01. Record the recovery effect of each algorithm on the same graph as the number of iterations increases.

Figure 5 lists the PSNR values for various iterations. For various iterative threshold class algorithms, when the number of iterations is greater than 35, good results can be maintained under low noise conditions, but if the number of iterations is less than 30, various algorithms based on gradient descent cannot achieve good results. As can be seen from Fig. 5, our proposed LISTA algorithm outperforms other algorithms with a sufficient number of iterations. Although LISTA algorithm is not as accurate as the FISTA algorithm in the case of too few iterations, the number of iterations in MR image recovery is generally sufficient, so this problem is acceptable.

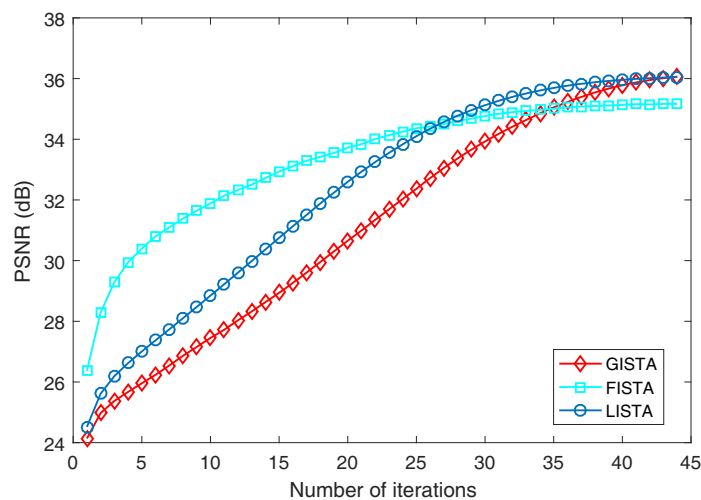


Figure 5. LISTA algorithm, GISTA algorithm, FISTA algorithm for the convergence analysis of the same MR image reconstruction under different iteration times.

5. CONCLUSIONS

This paper presents a new iterative threshold method based on log-sum algorithm for the first time. The new idea is embedded in two aspects: embedding log-sum norm regularization into the iterative threshold method; setting a new iterative threshold operator. In this paper, we demonstrate in detail the robustness of the algorithm compared to other algorithms. Experiments are performed to show the good results of our method. It can be clearly seen that the new iterative threshold algorithm has a significant improvement in some cases such as MR image recovery, compared to the L_p norm and the L_1 norm. The algorithm also has some shortcomings, i.e., the algorithm performs poorly at low iterations, which is related to the mathematical properties of log-sum norm. The iterative threshold operator needs more accurate estimation. When we process signals in real life, we often have more than one iterations, so this problem can be ignored.

ACKNOWLEDGMENT

This paper is supported by the National Key Laboratory of Communication Anti-jamming Technology (No. 614210202030217).

REFERENCES

1. Daubechies, I., M. Defrise, and C. D. Mol, "An iterative thresholding algorithm for linear inverse problems with a sparsity constraint," *Communications on Pure and Applied Mathematics*, Vol. 57, No. 11, 1413–1457, 2004.
2. Beck, A. and M. Teboulle, "A fast iterative shrinkage-thresholding algorithm for linear inverse problems," *SIAM Journal on Imaging Sciences*, Vol. 2, No. 1, 183–202, 2009.
3. Bioucasdias, J. M. and M. A. Figueiredo, "A new twist: Two-step iterative shrinkage/thresholding algorithms for image restoration," *IEEE Transactions on Image Processing*, Vol. 16, No. 12, 2992–3004, 2007.
4. Zuo, W., et al., "A generalized iterated shrinkage algorithm for non-convex sparse coding," *Proceedings of the IEEE International Conference on Computer Vision*, 2013.
5. Wang, P., P. Duan, and S. Xiong, "Image deblurring via fast generalized iterative shrinkage thresholding algorithm for lp regularization," *Journal of Wuhan University (Natural Science Edition)*, 2017.
6. Chartrand, R. and W. Yin, "Iteratively reweighted algorithms for compressive sensing," *Acoustics, Speech and Signal Processing*, 2008.
7. Zeng, J., et al., "Regularization: Convergence of iterative half thresholding algorithm," *IEEE Transactions on Signal Processing*, Vol. 62, No. 9, 2317–2329, 2013.
8. Cho, S., J. Wang, and S. Lee, "Handling outliers in non-blind image deconvolution," *International Conference on Computer Vision IEEE Computer Society*, 2011.
9. Dong, J., et al., "Blind image deblurring with outlier handling," *IEEE International Conference on Computer Vision (ICCV) IEEE*, 2017.
10. Rostami, M., O. Michailovich, and Z. Wang, "Image deblurring using derivative compressed sensing for optical imaging application," *IEEE Transactions on Image Processing*, Vol. 21, No. 7, 3139–3139, 2012.
11. Yin, X., L. Wang, H. Yue, and J. Xiang, "A new non-convex regularized sparse reconstruction algorithm for compressed sensing magnetic resonance image recovery," *Progress In Electromagnetics Research C*, Vol. 87, 241–253, 2018.
12. Rao, B. D. and K. Kreutz-Delgado, "An affine scaling methodology for best basis selection," *IEEE Transactions on Signal Processing*, Vol. 47, No. 1, 187–200, 2002.
13. Shen, Y., J. Fang, and H. Li, "Exact reconstruction analysis of log-sum minimization for compressed sensing," *IEEE Signal Processing Letters*, Vol. 20, No. 12, 1223–1226, 2013.

14. Deng, Y., et al., "Low-rank structure learning via log-sum heuristic recovery," *5th Pacific Rim Conference on Multimedia*, 1012–1919, Mathematics, 2010.
15. Candes, E. and T. Tao, "Near optimal signal recovery from random projections: Universal encoding strategies," *IEEE Trans. Inf. Theory*, Vol. 52, No. 12, 5406–5425, 2006.
16. Donoho, D. L., "For most large underdetermined systems of linear equations the minimal l_1 -norm solution is also the sparsest solution," *Communications on Pure and Applied Mathematics*, Vol. 59, No. 7, 907–C934, 2006.